SECTION 4

ANALYTICAL PREDICTION OF RESPONSE

A mathematical model of equipment supported by wire rope isolators is developed for the analytical prediction of dynamic response. The model accounts only for in - plane response as if the excitation consists of only components in a vertical plane and the system exhibits no eccentricities. Furthermore, three assumptions are made:

1. The possible interaction between vertical and horizontal components of force developed at a wire rope isolator is negligible. Each isolator is modeled by two independent hysteretic elements (springs) which exhibit the characteristics identified in section 2. The two springs are placed in the vertical and horizontal directions at each location of wire rope isolator.
2. The rotational stiffness of wire rope isolators is negligible.
3. The equipment is rigid. This assumption can be easily relaxed.

Figure 4-1 shows the model of a rigid equipment supported by wire rope isolators. The springs representing wire rope isolators are symmetrically placed at distance a from the center of mass and at the same height h below the center of mass. The degrees of freedom are selected to be the horizontal, u_x, and vertical u_z, displacements and rotation, θ, of the center of mass.

4.1 Equations of Motion for Large Rotations

The equations of motion are first derived by considering large rotations and subsequently reduced to their geometrically linear form (small rotations).

Two orthogonal coordinate systems are defined. The first, XZ, is fixed in time and defined to have its origin at the initial position of static equilibrium (at time t=0) of the center of mass. The second, X´Z´, is moving with the center of mass as illustrated in Figure 4-1. The degrees of freedom are the translations, u_x and u_z of the center of mass with respect to the initial position (CM in Figure 4-1) and its clockwise rotation θ. It should be noted that in classical terminology, coordinates XZ are refer to as reference or material or configuration or Lagrangian coordinates and coordinates X´Z´ are refer to as present or spatial or Eulerian coordinates.

A point i having coordinates (X'_i, Z'_i) in the moving system can be defined in terms of coordinates in the fixed-initial system by the following transformation:

$$\begin{bmatrix} X_i \\ Z_i \end{bmatrix} = \begin{bmatrix} u_x \\ u_z \end{bmatrix} + \begin{bmatrix} \cos\theta & \sin\theta \\ -\sin\theta & \cos\theta \end{bmatrix} \begin{bmatrix} X'_i \\ Z'_i \end{bmatrix} \tag{4-1}$$

The displacements of point i with respect to its initial position are

$$\begin{bmatrix} u_{xi} \\ u_{zi} \end{bmatrix} = \begin{bmatrix} X_i \\ Z_i \end{bmatrix} - \begin{bmatrix} X'_i \\ Z'_i \end{bmatrix} \tag{4-2}$$

At time t=0 the two systems are identical and therefore $X_i=X'_i$ and $Z_i=Z'_i$.

The displacements of some points of interest are derived from equations 4-1 and 4-2 and given below. These points are B1 and B2 at the bearing level and T2 at the top level of the equipment (see Figure 4-2). These points have the following coordinates with respect to the moving system:

$X'_{B1}=-a$, $X'_{B2}=a$, $Z'_{B1}=Z'_{B1}=-h$, $X'_{T2}=b$, $Z'_{T2}=h_T$.

$$u_{xB1} = u_x - a(\cos\theta - 1) - h.\sin\theta \tag{4-3}$$

$$u_{zB1} = u_z + h(1 - \cos\theta) + a.\sin\theta \tag{4-4}$$

$$u_{xB2} = u_x + a(\cos\theta - 1) - h.\sin\theta \tag{4-5}$$

$$u_{zB2} = u_z + h(1 - \cos\theta) - a.\sin\theta \tag{4-6}$$

$$u_{xT2} = u_x + b(\cos\theta - 1) + h_T.\sin\theta \tag{4-7}$$

$$u_{zT2} = u_z - h_T(1 - \cos\theta) - b.\sin\theta \tag{4-8}$$

The equations of motion of the equipment are derived from dynamic equilibrium using the free body diagram of Figure 4-2:

$$m\ddot{u}_x + 2F_{x1} + 2F_{x2} = -m\ddot{u}_{gx} \tag{4-9}$$

$$m\ddot{u}_z + 2F_{z1} + 2F_{z2} + W = -m\ddot{u}_{gz} \tag{4-10}$$

$$I_o\ddot{\theta} - 2F_{x1}D_{z1} - 2F_{x2}D_{z2} + 2F_{z1}D_{x1} - 2F_{z2}D_{x2} = 0 \tag{4-11}$$

in which $I_o = mr^2$ is the moment of inertia of the equipment about the horizontal axis passing through the center of mass, r = radius of gyration, m = mass, W = weight and $\ddot{u}_{gx}$ and $\ddot{u}_{gz}$ are the horizontal and vertical components of the input motion, respectively. Furthermore, F_{x1} and F_{x2} are the spring forces in the horizontal direction at points B1 and B2 which are given by equations 2-1 and 2-2 for displacement $U = u_{xB1}$ and $U = u_{xB2}$, respectively. Moreover F_{z1} and F_{z2} are the spring forces in the vertical direction at points B1 and B2 which are given by equations 2-5 to 2-7 and 2-2 for vertical displacement $U = u_{zB1}$ and $U = u_{zB2}$, respectively. Distances D_{x1}, D_{x2}, D_{z1} and D_{z2} represent the horizontal and vertical arms of isolator forces with respect to the center of mass and are given by the following expressions:

$$D_{x1} = a.\cos\theta + h.\sin\theta \tag{4-12}$$

$$D_{x2} = a.\cos\theta - h.\sin\theta \tag{4-13}$$

$$D_{z1} = -a.\sin\theta + h.\cos\theta \tag{4-14}$$

$$D_{z2} = a.\sin\theta + h.\cos\theta \tag{4-15}$$

Equations 2-1, 2-2, 2-5 to 2-7, 4-3 to 4-6 and 4-9 to 4-15 form a system of ten first order differential equations. Initial conditions are zero except for displacement u_z which is equal to the static vertical displacement of the isolators due to the weight of the equipment. Numerical solutions were derived by use of Gear's implicit multistep integration scheme with adaptive time step (Gear 1971, IMSL 1987).

4.2 Equations of Motion for Small Rotations

For small rotations, $\sin\theta$ and $\cos\theta$ may be expanded in binomial series. Correct to $O(\theta^2)$, $\cos\theta$ and $\sin\theta$ may be replaced by 1 and θ, respectively. The error involved in such an approximation does not exceed 2% of exact for values of θ up to 0.2 rad (11.4 degrees). In all of the tests presented in section 3 the angle of rotation did not exceed this limit. Accordingly, the geometrically linear equations of motion introduce errors which are insignificant for practical purposes.

The geometrically linear form of equations 4-3 to 4-15 is:

$$u_{xB1} = u_{xB2} = u_{xb} = u_x - h.\theta \tag{4-16}$$

$$u_{zB1} = u_z + a.\theta \tag{4-17}$$

$$u_{zB2} = u_z - a.\theta \tag{4-18}$$

$$D_{x1} = a + h.\theta \tag{4-19}$$

$$D_{x2} = a - h.\theta \tag{4-20}$$

$$D_{z1} = -a.\theta + h \tag{4-21}$$

$$D_{z2} = a.\theta + h \tag{4-22}$$

As a result of equation 4-16,

$$F_{x1} = F_{x2} = F_x \tag{4-23}$$

and the equations of motion modify to

$$m\ddot{u}_x + 4F_x = -m\ddot{u}_{gx} \tag{4-23}$$

$$m\ddot{u}_z + 2F_{z1} + 2F_{z2} + W = -m\ddot{u}_{gz} \tag{4-25}$$

$$I_o\ddot{\theta} - 4F_x h + 2F_{z1}(a + h\theta) - 2F_{z2}(a - h\theta) = 0 \tag{4-26}$$

In these equations, F_x is given by equations 2-1 and 2-2 with $U = U_{xb}$ and F_{z1} and F_{z2} are given by equations 2-1, 2-5 to 2-7 with $U = u_{zB1}$ (eq. 4-17) and $U = u_{zB2}$ (eq. 4-18), respectively.

Integration of the geometrically linear equations of motion resulted in responses which were almost identical to those obtained from the geometrically nonlinear equations. This was the case for all analyzed systems, some of which underwent rotations of up to 0.2 rad.

The geometrically linear equations of motion are useful in the development of a simplified analysis procedure which can be used together with floor response spectra to obtain estimates of the peak response.

4.3 Simplified Analysis Procedure

A simplified analysis procedure is developed by assuming that each wire rope isolator may be represented by two linear springs of stiffness K_x in the horizontal direction and stiffness K_z in the vertical direction. Furthermore, the energy dissipation is accounted for by the use of equivalent viscous damping ratios in modal analysis. Forces F_x, F_{z1} and F_{z2} are expressed as

$$F_x = K_x(u_x - h\theta) \tag{4-27}$$

$$F_{z1} = K_z(u_z + a\theta) \tag{4-28}$$

$$F_{z2} = K_z(u_z - a\theta) \tag{4-29}$$

Substituting equations 4-27 to 4-29 into 4-24 to 4-26, the linear equations of motion are derived after droping higher order terms:

$$m\ddot{u}_x + 4K_x u_x - 4K_x h\theta = -m\ddot{u}_{gx} \tag{4-30}$$

$$m\ddot{u}_z + 4K_z u_z + W = -m\ddot{u}_{gz} \tag{4-31}$$

$$I_o\ddot{\theta} - 4K_x h u_x + (4K_z a^2 + 4K_x h^2)\theta = 0 \tag{4-32}$$

In these equations u_z is decoupled from the other degrees of freedom because the system has no eccentricities. Accordingly, the analysis for vertical excitation may be performed independently of that for horizontal excitation.

Concentrating on the coupled horizontal - rocking response, equations 4-30 and 4-32 are expressed in the following matrix form upon division by mass m:

$$[I]\{\ddot{U}\} + [K]\{U\} = -\{R\}\ddot{u}_{gx} \tag{4-33}$$

where [I] is the identity matrix,

$$\{U\} = \begin{Bmatrix} u_x \\ r\theta \end{Bmatrix}, \quad \{R\} = \begin{Bmatrix} 1 \\ 0 \end{Bmatrix} \tag{4-34}$$

and

$$[K] = \begin{bmatrix} \omega_x^2 & -\omega_x^2\left(\frac{h}{r}\right) \\ -\omega_x^2\left(\frac{h}{r}\right) & \omega_x^2\left(\frac{h}{r}\right)^2 + \omega_z^2\left(\frac{a}{r}\right)^2 \end{bmatrix} \tag{4-35}$$

In the above equation

$$\omega_x = \left(\frac{4K_x}{m}\right)^{1/2}, \quad \omega_z = \left(\frac{4K_z}{m}\right)^{1/2} \tag{4-36}$$

are the roll and vertical frequencies of the isolated equipment, respectively.

Equations 4-33 may be solved for the modal properties of the linearized system which together with representative damping ratios may be used to obtain estimates of the peak response of the system to horizontal excitation. In free vibration, $\ddot{u}_{gx} = 0$ and

$$\{U\} = \{\phi_n\} e^{i\omega_n t} \tag{4-37}$$

in which ω_n = frequency of free vibration and ϕ_{xn} and $\phi_{\theta n}$ are elements of mode shape $\{\phi_n\}$ corresponding to u_x and $r\theta$, respectively. Equation 4-33 takes the form:

$$\begin{bmatrix} \omega_x^2 - \omega_n^2 & -\omega_x^2\left(\frac{h}{r}\right) \\ -\omega_x^2\left(\frac{h}{r}\right) & \omega_x^2\left(\frac{h}{r}\right)^2 + \omega_z^2\left(\frac{a}{r}\right)^2 - \omega_n^2 \end{bmatrix} \begin{Bmatrix} \phi_{xn} \\ \phi_{\theta n} \end{Bmatrix} = \begin{Bmatrix} 0 \\ 0 \end{Bmatrix} \tag{4-38}$$

The requirement for nontrivial solution gives the characteristic equation from where the frequencies of the coupled system, ω_1 and ω_2, may be calculated:

$$\omega_n^4 - \left[\omega_x^2\left(1 + \left(\frac{h}{r}\right)^2\right) + \omega_z^2\left(\frac{a}{r}\right)^2\right]\omega_n^2 + \omega_x^2\omega_z^2\left(\frac{a}{r}\right)^2 = 0\,, \quad n = 1,2 \tag{4-39}$$

With the frequencies calculated from equation 4-39, equation 4-38 is used to obtain the mode shapes.

The calculation of peak response values may be performed by the modal analysis approach (Clough 1975). Applying the transformation

$$\{U\} = [\Phi]\{y\} \tag{4-40}$$

to equation 4-33, using the orthogonality conditions and introducing modal damping one obtains

$$\ddot{y}_n + 2\xi_n\omega_n\dot{y}_n + \omega_n^2 y_n = -\frac{[\Phi]^T\{R\}\ddot{u}_{gx}}{[\Phi]^T[\Phi]}\,, \quad n = 1,2 \tag{4-41}$$

In the above equations $[\Phi]$ is a matrix containing in its columns the two mode shapes and ξ_n is the damping ratio in

mode n. Peak modal responses are calculated from response spectra of the floor motion:

$$\max y_n = \frac{[\Phi]^T\{R\}}{[\Phi]^T[\Phi]} S_d(\omega_n, \xi_n) \tag{4-42}$$

$$\max \ddot{y}_{n\,TOTAL} = \frac{[\Phi]^T\{R\}}{[\Phi]^T[\Phi]} S_a(\omega_n, \xi_n) \tag{4-43}$$

where S_d and S_a are, respectively, the spectral displacement and spectral acceleration of the floor motion for frequency ω_n and damping ratio ξ_n. Peak responses for each mode are calculated by use of equation 4-40 and then combined by the square-root-sum-squares (SRSS) combination rule.

The simplified procedure is very useful in obtaining quick estimates of the peak response. It requires, however the effective stiffnesses of the wire rope isolators and the effective damping ratio of the system. The effective stiffness may be obtained from experimental force - displacement loops of the isolators. This requires the employment of an iterative procedure to first calculate displacements and subsequently estimate stiffnesses and refine calculations. The effective damping ratio, however, can not be a-priori selected. A nonlinear dynamic analysis for harmonic excitation may be performed and calculated moment - rotation loops may be used to obtain values of effective damping ratio (see section 3.3). Otherwise, damping must be selected with conservatism and based on experience.

4.4 Comparison of Experimental and Analytical Results

Comparisons of experimental and analytical time histories of response of system 1 are presented in Figures 4-3 to 4-21. All analyses were based on the geometrically nonlinear formulation of section 4.1. Analyses with the geometrically linear equations of section 4.2 gave almost identical results. The parameters in the analytical model were W = 400 lbs (1784 N), r = 22.83 in. (580 mm), a = 9.125 in. (231.8 mm), h = 40.2 in. (1021 mm) and h_1 = 36.2 in. (919.5 mm).

The analytical time history results are in good agreement with the experimental results. The content in frequency is reproduced very well, however the displacements are in many cases overpredicted. A number of factors may be contributing to this, with the two dominating ones being the neglect of interaction and lesser energy dissipation in the mathematical model of the isolators.

Peak response values of system 1 as computed by time history analysis and by the simplified method are compared to experimental results in Table 4-I. The simplified method required estimates of isolator stiffnesses and damping ratio. They were determined by the following procedure. The system was numerically analyzed for harmonic excitation and loops of moment - rotation were determined (see section 3.3, equations 3-1 and 3-2). From these loops, which are shown in Figure 4-22, values of effective period and equivalent viscous damping ratio (equations 3-3 and 3-4) were calculated. Furthermore,

representative values of the vertical isolators stiffness, K_z, were determined from

$$K_r = \frac{M}{\theta} = 4K_z a^2 \qquad (4\text{-}44)$$

These quantities are listed in Table 4-II as function of the amplitude of rotation ($2\theta a$). Moreover, representative values of the isolator horizontal stiffness, K_x, were determined from experimental lateral force - displacement loops (see section 2, Fig. 2-4).

The analysis was performed by assuming a representative value of rotation, θ, then selecting appropriate values of vertical stiffness, K_z, and damping ratio, ξ, and performing response spectrum analysis (section 4.3). Subsequently, the calculated value of rotation was used to improve the estimates of K_z and ξ using the data of Table 4-II and the analysis was repeated. This iterative process was applied for four of the floor excitations using the spectra of Figures 3-5 to 3-10. The calculated system characteristics are presented in Table 4-III, while the response is presented in Table 4-I. It should be noted that the damping factor in the second mode was not known and was assumed to be equal to that in the first mode.

The results of Table 4-I demonstrate good agreement between analytical and experimental peak response values. It may be stated that the simplified method is sufficiently accurate to represent a useful design tool.

Table 4-I - Comparison of Experimental and Analytical Peak Response Values (1 in.= 25.4 mm).

	TAFT N21E GROUND MOTION			TAFT N21E 7th FLOOR		
	Experiment	Time History	Simplified Method	Experiment	Time History	Simplified Method
Top Horizontal Acceleration (g)	0.220	0.233	0.248	0.625	0.648	0.706
Top Horizontal Displacement (in)	1.211	1.214	1.620	4.163	4.449	4.906
Isolator Horizontal Displacement (in)	0.122	0.100	0.182	0.302	0.412	0.529
Isolator S Vertical Displacement (in)	0.247	0.247	0.262	1.031	1.001	0.799
Isolator N Vertical Displacement (in)	0.198	0.186	0.262	0.806	0.977	0.799

Table 4-I – Continued.

	EL CENTRO S00E GROUND MOTION			EL CENTRO S00E 7th FLOOR		
	Experiment	Time History	Simplified Method	Experiment	Time History	Simplified Method
Top Horizontal Acceleration (g)	0.546	0.516	0.616	1.057	0.872	0.984
Top Horizontal Displacement (in)	4.753	4.868	4.736	11.860	11.762	15.220
Isolator Horizontal Displacement (in)	0.401	0.467	0.505	0.749	1.182	1.300
Isolator S Vertical Displacement (in)	1.145	1.137	0.770	3.279	3.070	2.534
Isolator N Vertical Displacement (in)	0.844	0.914	0.770	2.705	3.133	2.534

Table 4-II - Properties of System 1 Extracted from Moment-Rotation Loops of Fig.4-22 (1 in.= 25.4 mm, 1 Kip= 4.46 kN).

M/a (Kips)	2θa (in.)	K_z (Kip/in)	Effective Period (sec)	Equivalent Viscous Damping Ratio
0.423	0.590	0.360	0.86	0.132
0.600	1.000	0.300	0.94	0.098
0.730	1.513	0.241	1.04	0.074

Table 4-III - Characteristics of System 1 used in Simplified Analysis (1 in.= 25.4 mm, 1 Kip= 4.46 kN).

EXCITATION	K_x (Kip/in)	K_z (Kip/in)	ω_x (r/s)	ω_z (r/s)	T_1 (sec)	T_2 (sec)	ξ_1	ξ_2
Taft Ground	0.179	0.360	26.29	37.29	0.88	0.12	0.15	0.15
Taft 7th Floor	0.179	0.300	26.29	34.04	0.96	0.12	0.10	0.10
El Centro Ground	0.179	0.300	26.29	34.04	0.96	0.12	0.10	0.10
El Centro 7th Floor	0.179	0.100	26.29	19.65	0.64	0.12	0.05	0.05

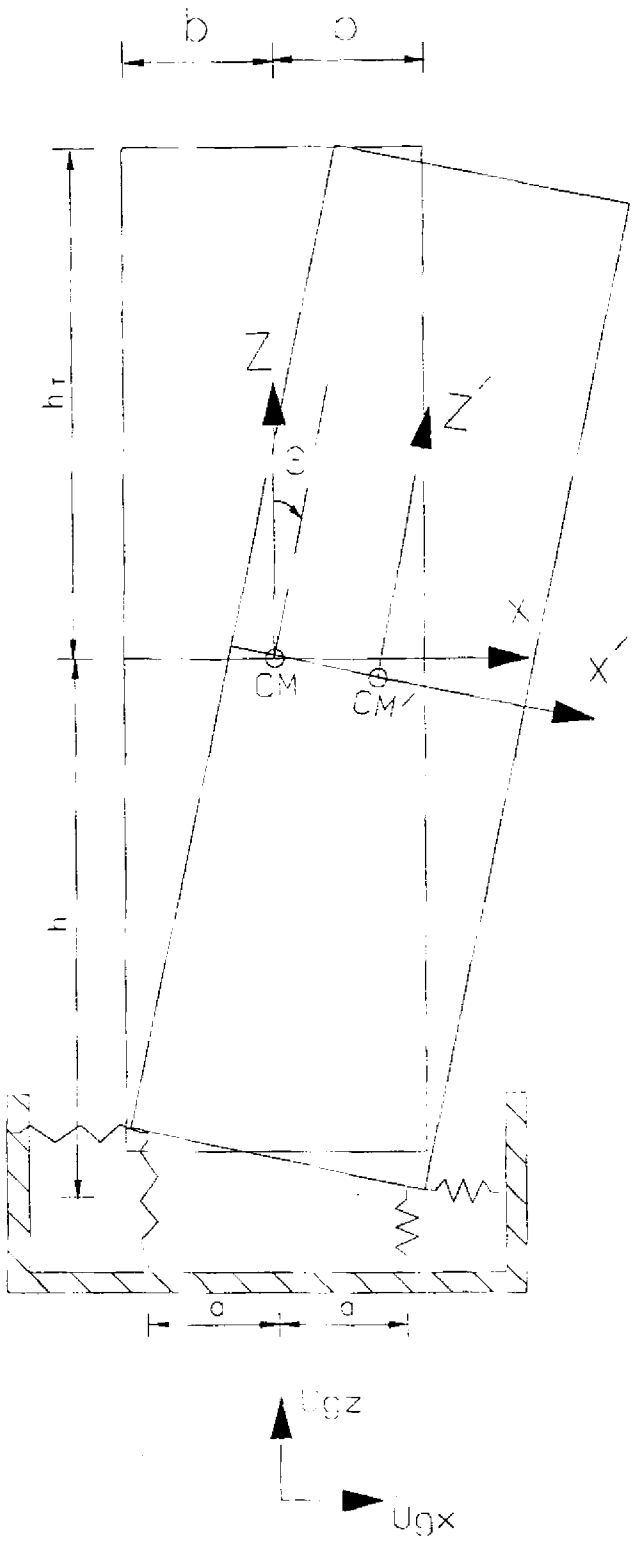

Figure 4-1 Model of Equipment Supported by Wire Rope Isolators.

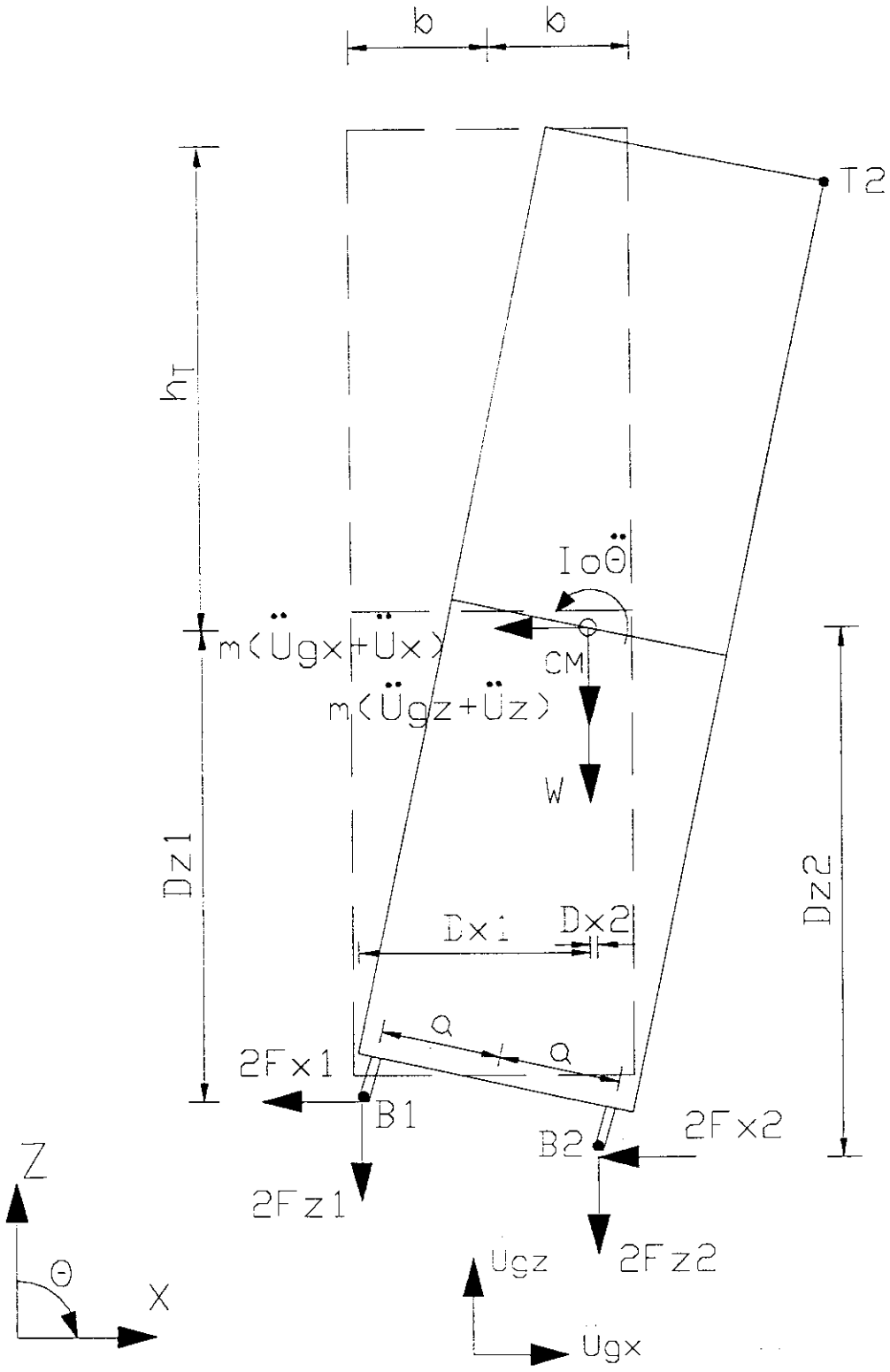

Figure 4-2 Free Body Diagram of Equipment.

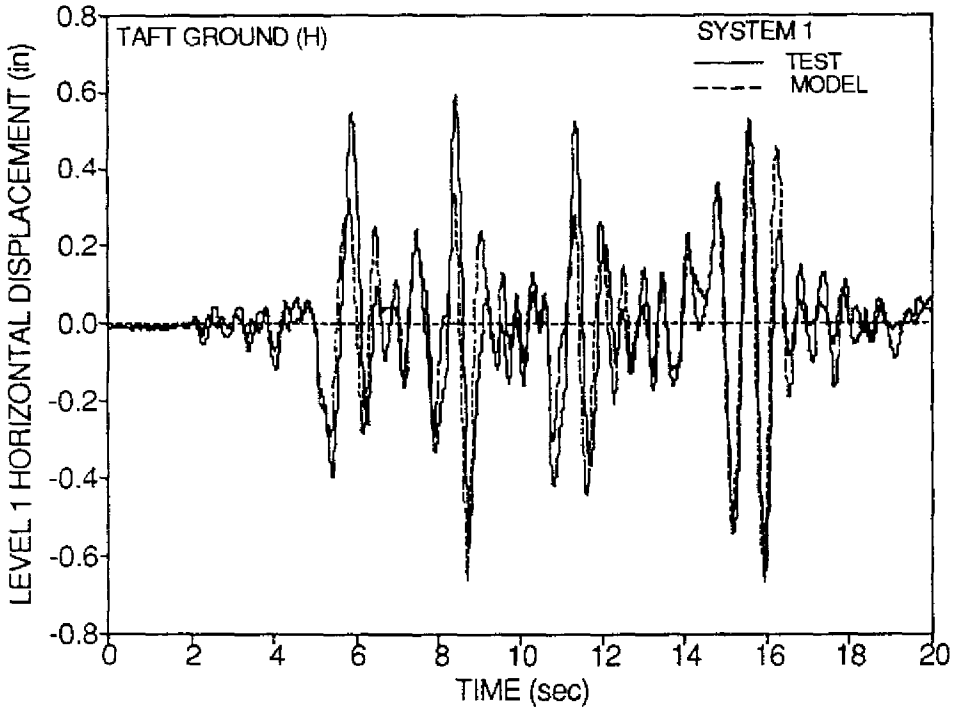

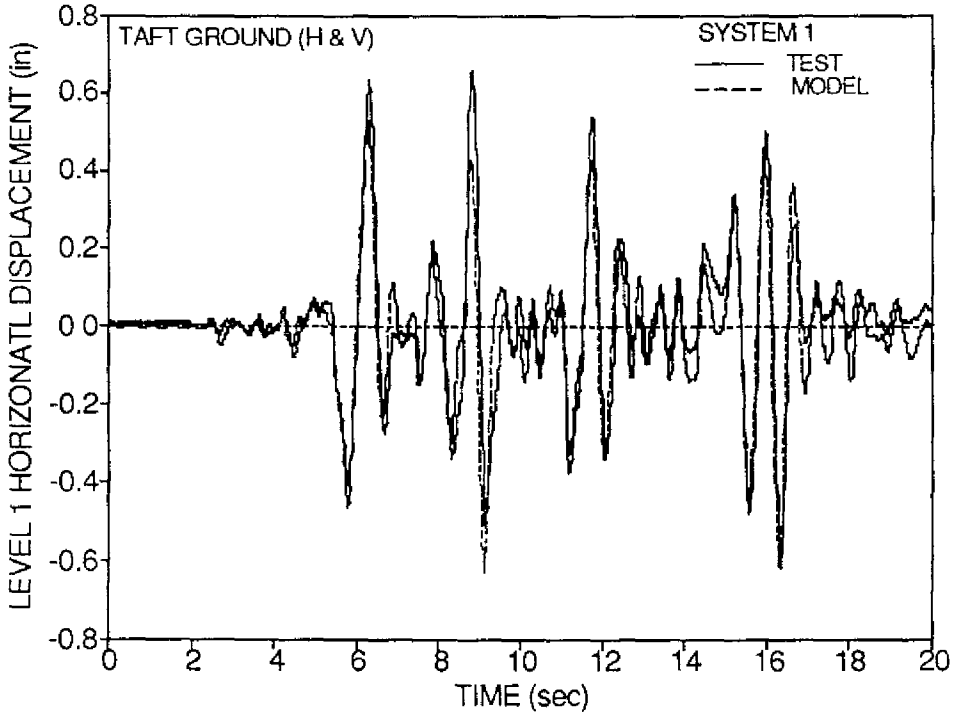

Figure 4-3 Comparison of Experimental and Analytical Time Histories of Horizontal Displacement of Level 1 for Taft Ground Motion (1 in.= 25.4 mm).

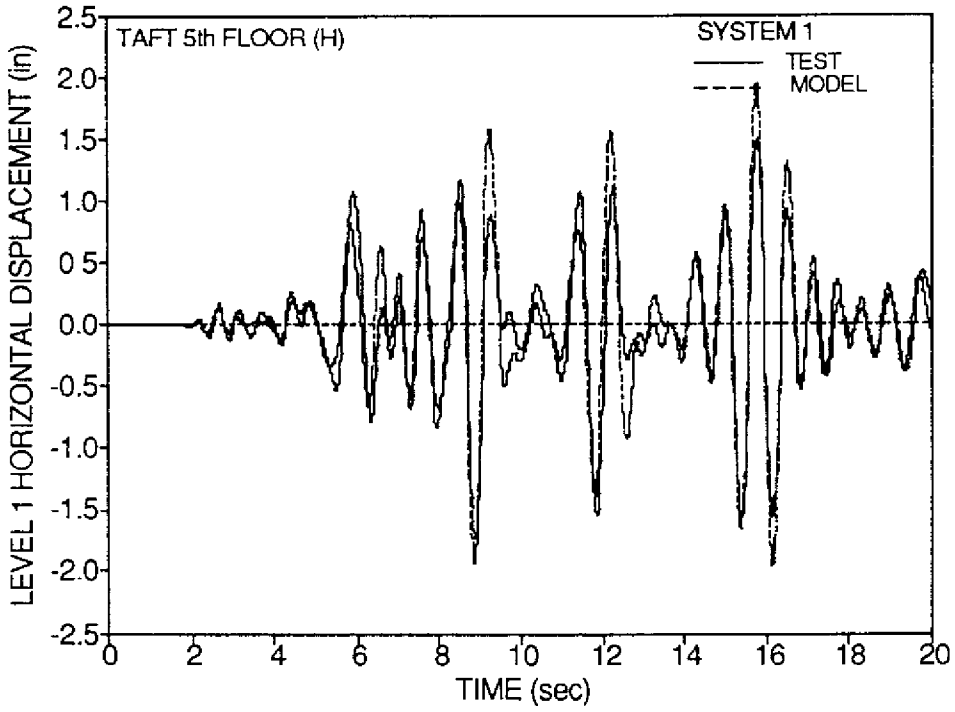

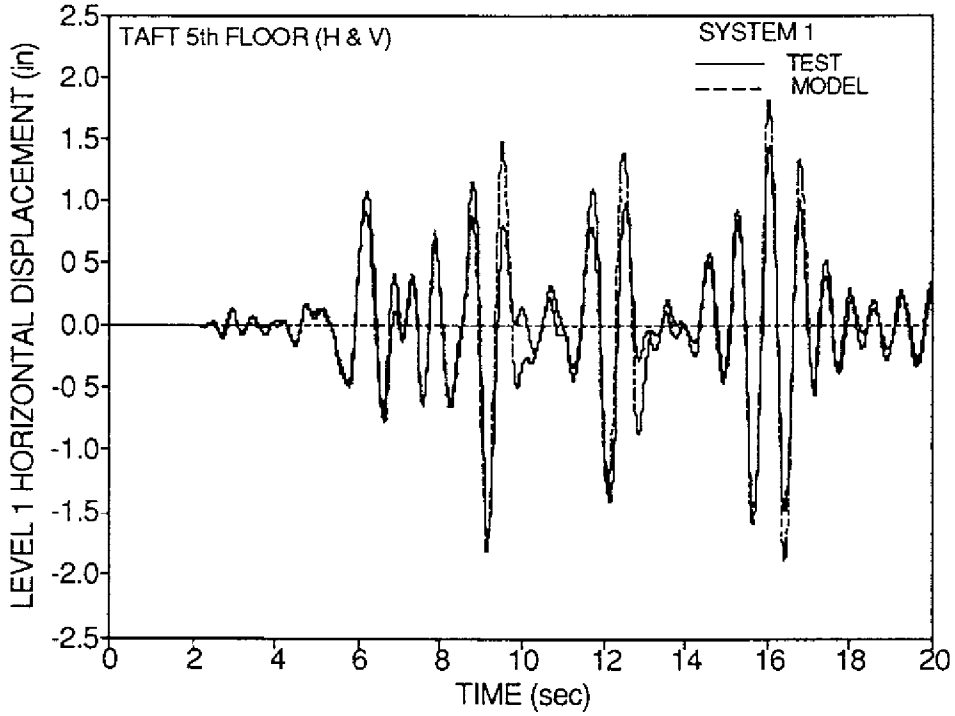

Figure 4-4 Comparison of Experimental and Analytical Time Histories of Horizontal Displacement of Level 1 for Taft 5th Floor Motion (1 in.= 25.4 mm).

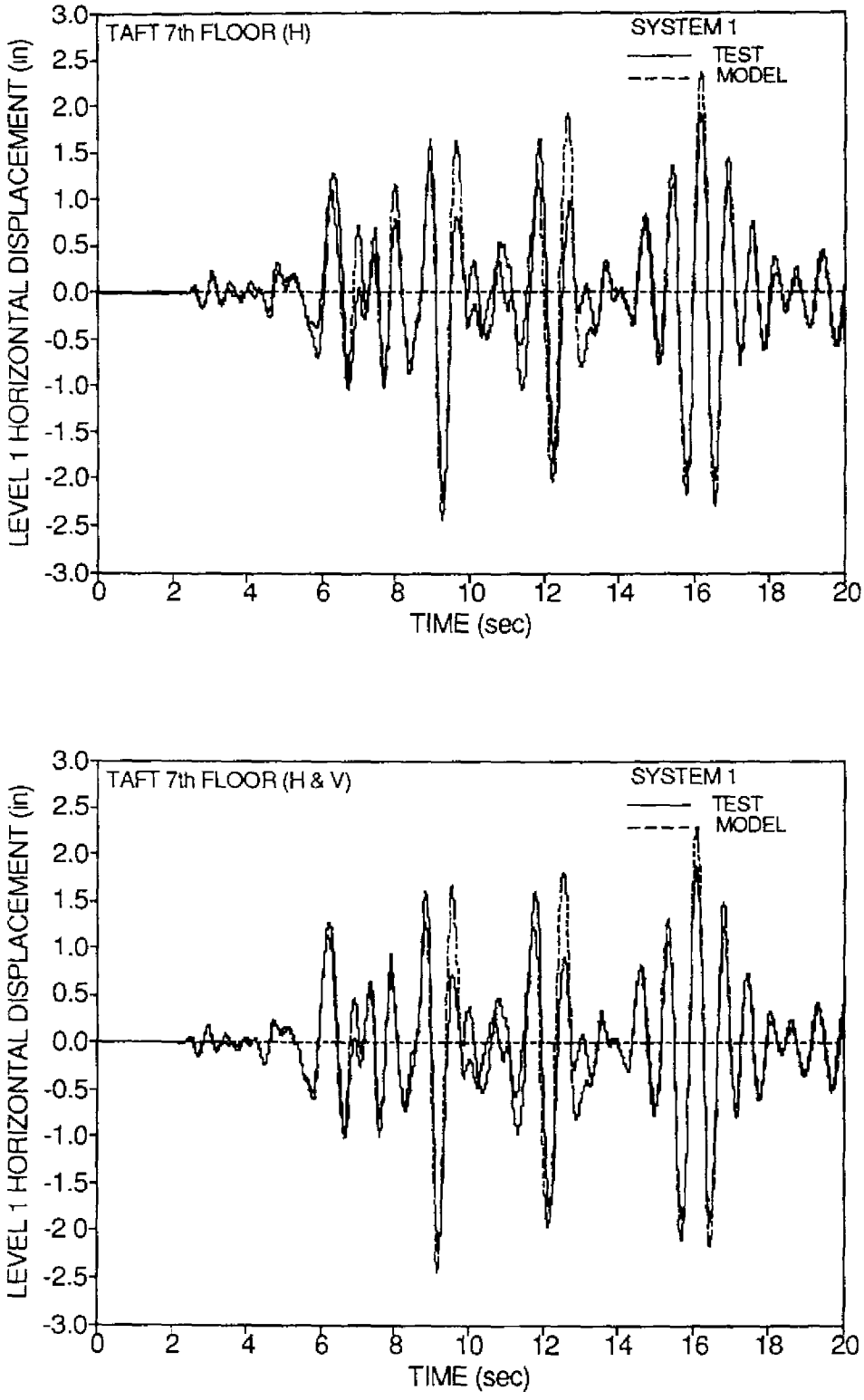

Figure 4-5 Comparison of Experimental and Analytical Time Histories of Horizontal Displacement of Level 1 for Taft 7th Floor Motion (1 in.= 25.4 mm).

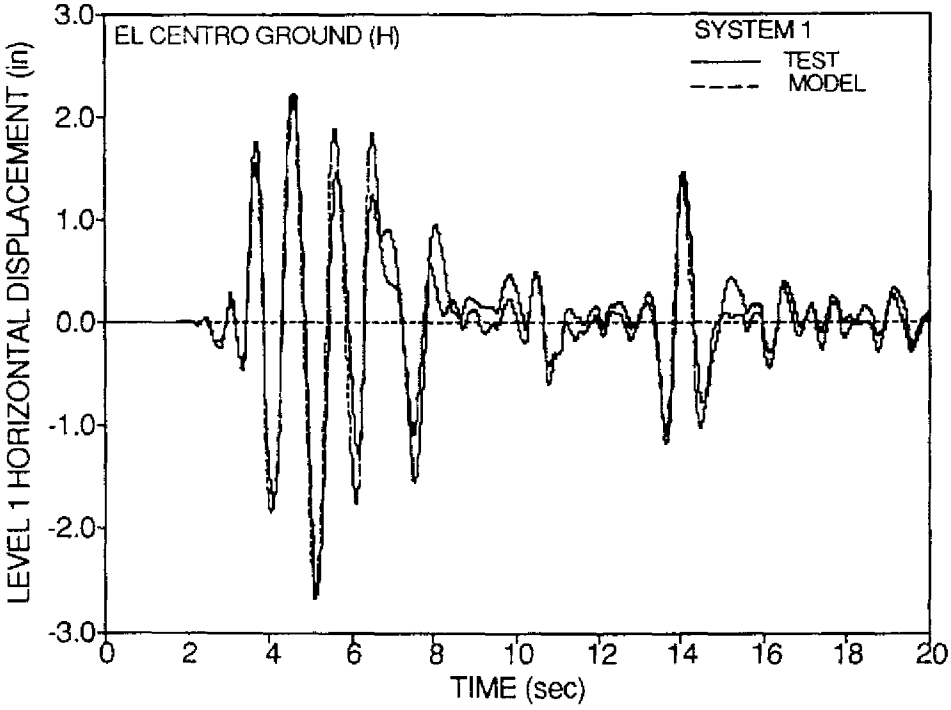

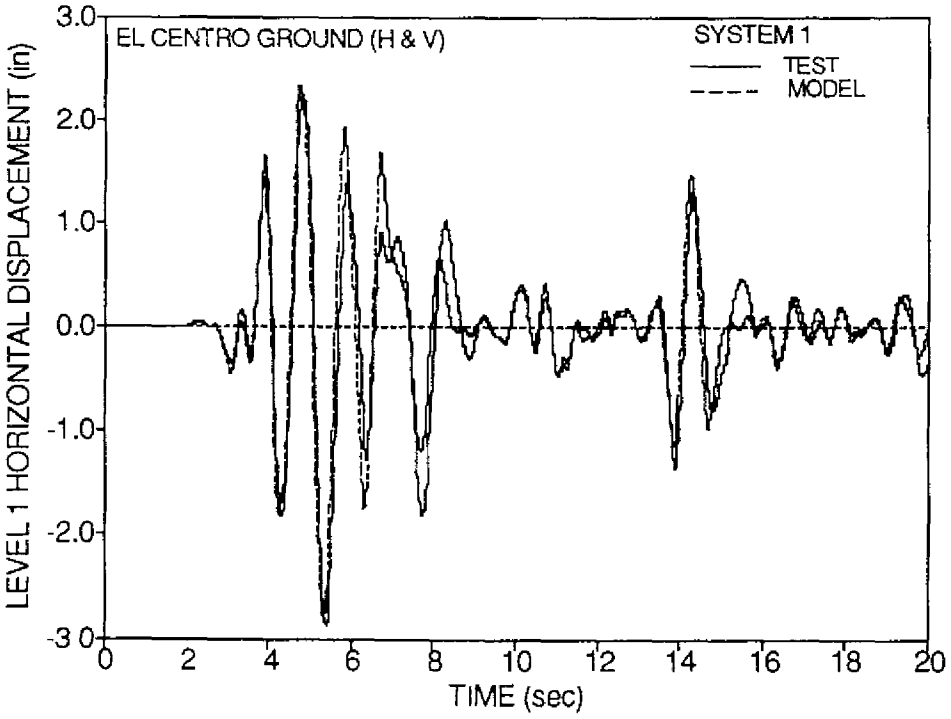

Figure 4-6 Comparison of Experimental and Analytical Time Histories of Horizontal Displacement of Level 1 for El Centro Ground Motion (1 in.= 25.4 mm).

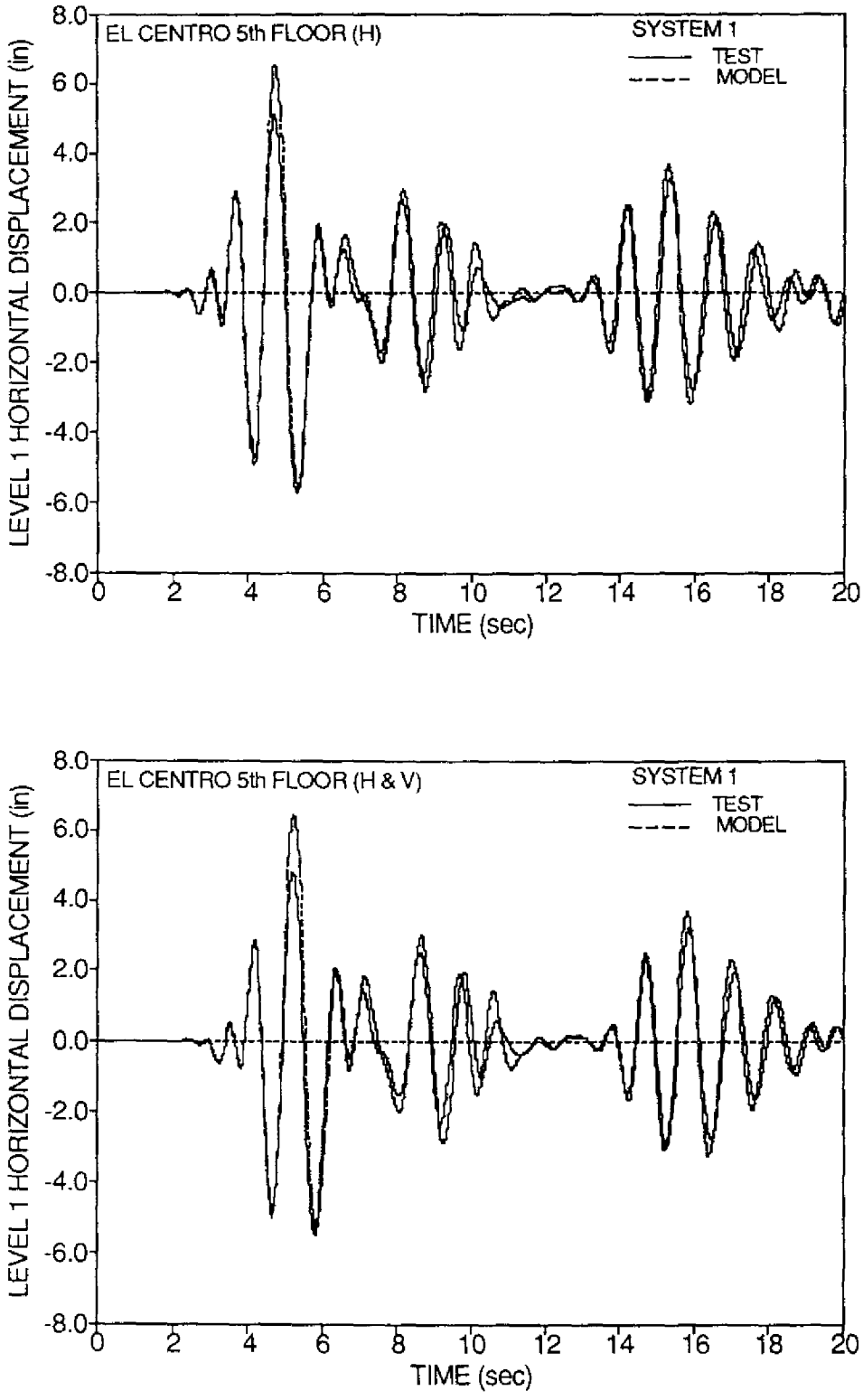

Figure 4-7 Comparison of Experimental and Analytical Time Histories of Horizontal Displacement of Level 1 for El Centro 5th Floor Motion (1 in.= 25.4 mm).

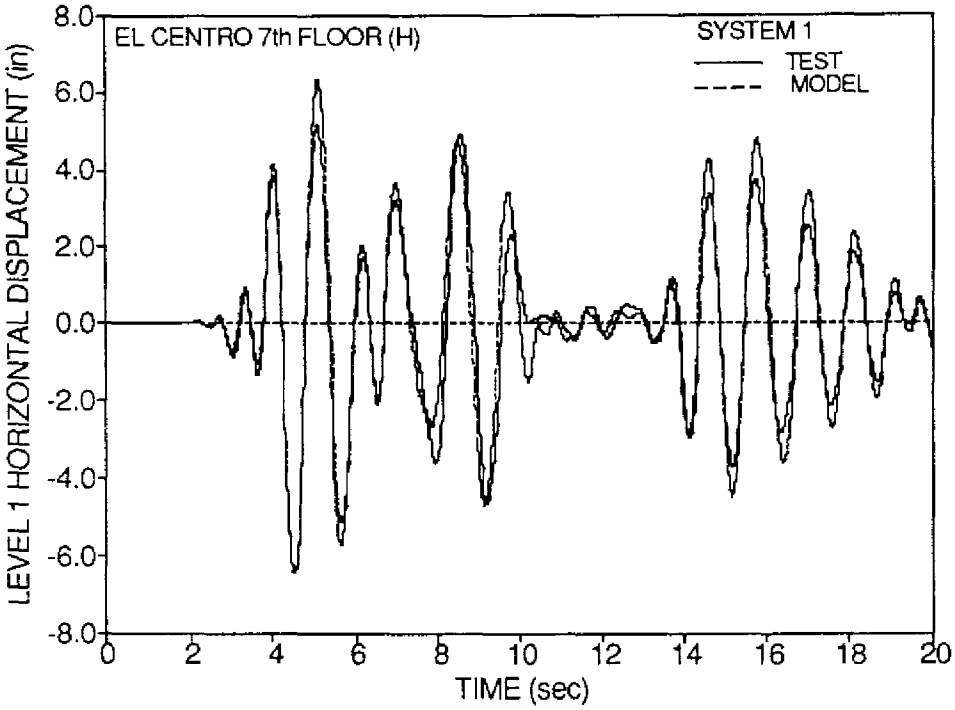

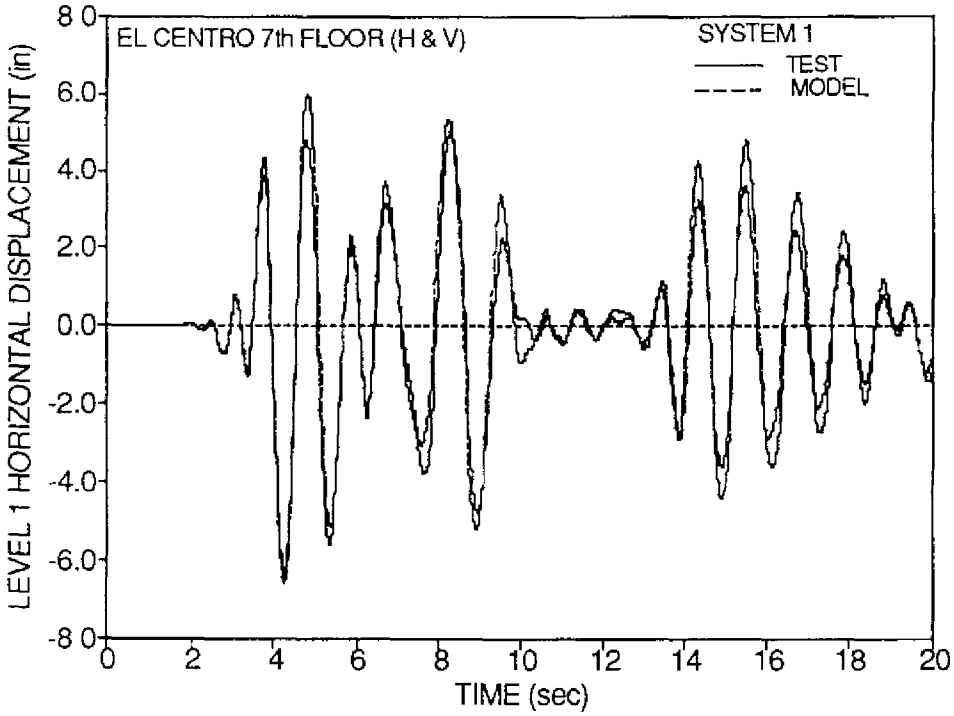

Figure 4-8 Comparison of Experimental and Analytical Time Histories of Horizontal Displacement of Level 1 for El Centro 7th Floor Motion (1 in.= 25.4 mm).

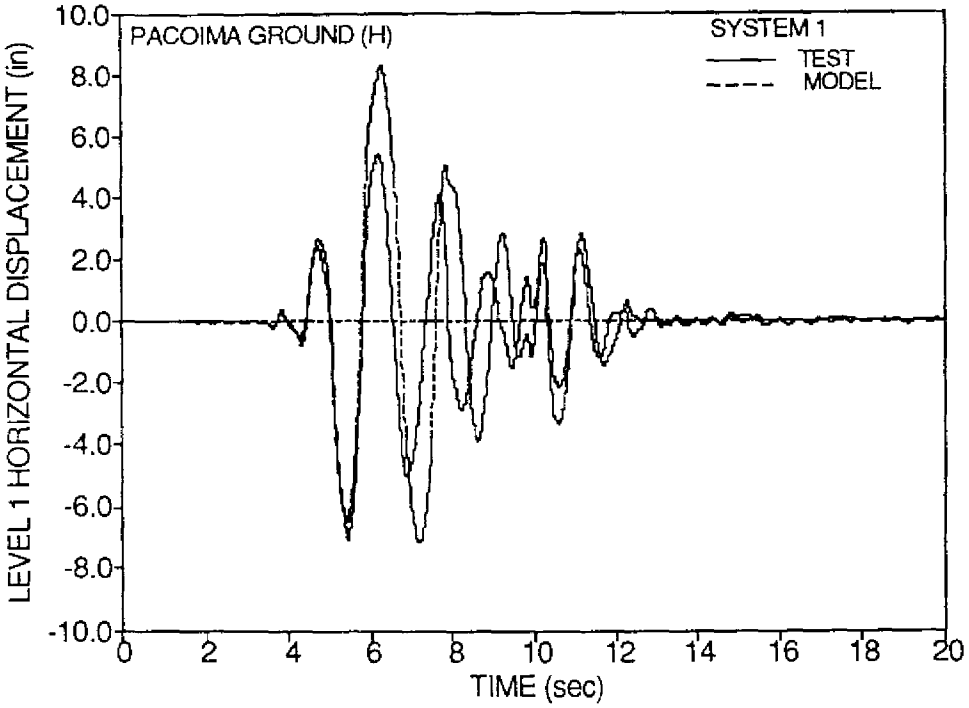

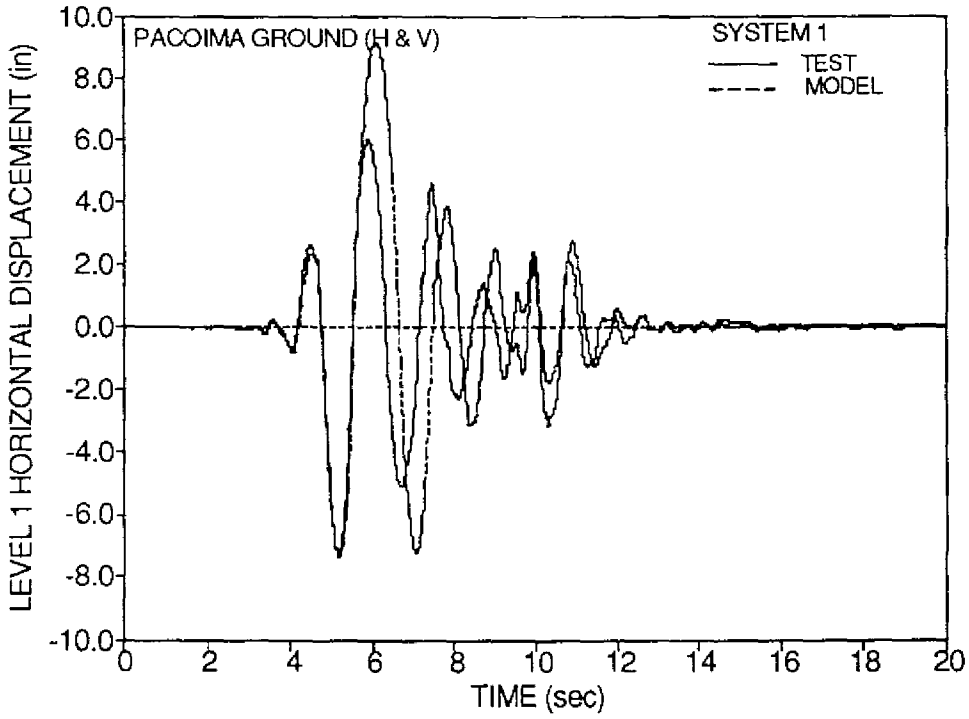

Figure 4-9 Comparison of Experimental and Analytical Time Histories of Horizontal Displacement of Level 1 for Pacoima Ground Motion (1 in.= 25.4 mm).

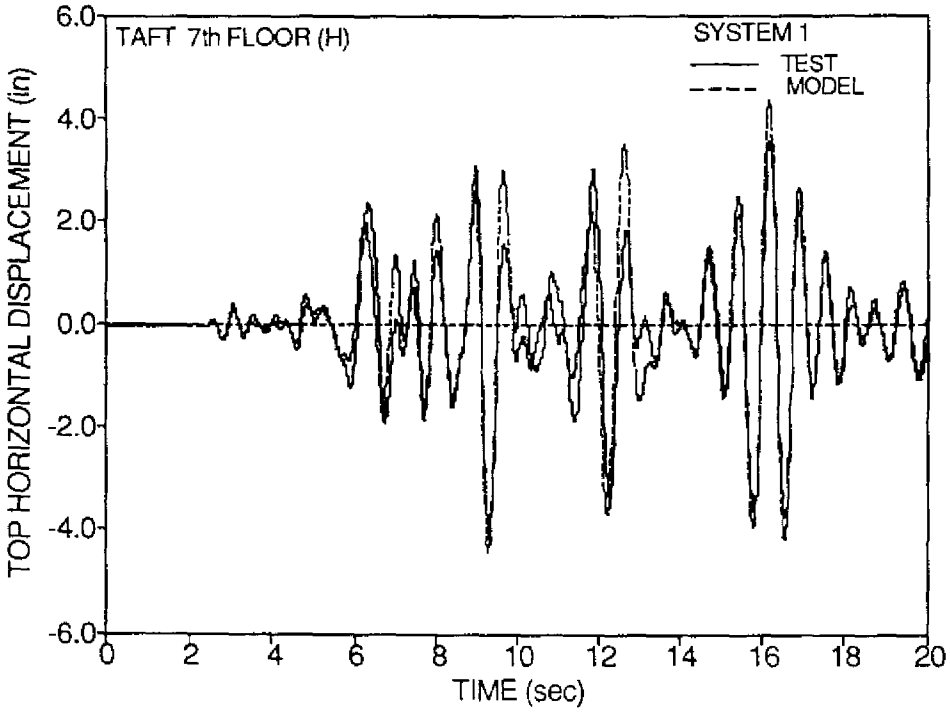

Figure 4-10 Comparison of Experimental and Analytical Time Histories of Horizontal Displacement of Top for Taft 7th Floor Motion (1 in.= 25.4 mm).

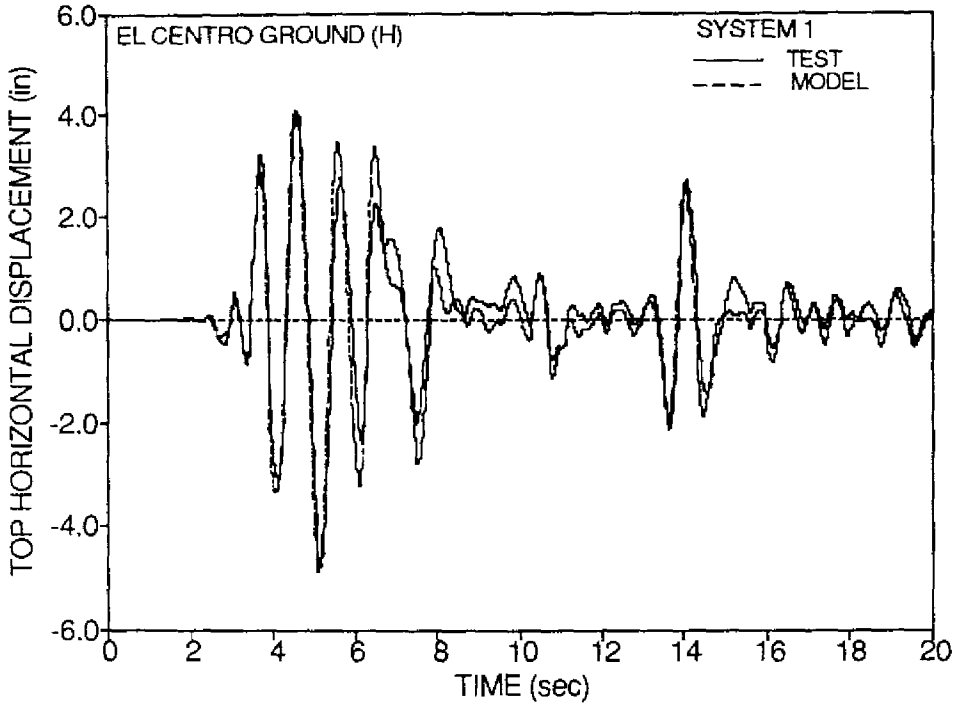

Figure 4-11 Comparison of Experimental and Analytical Time Histories of Horizontal Displacement of Top for El Centro Ground Motion (1 in.= 25.4 mm).

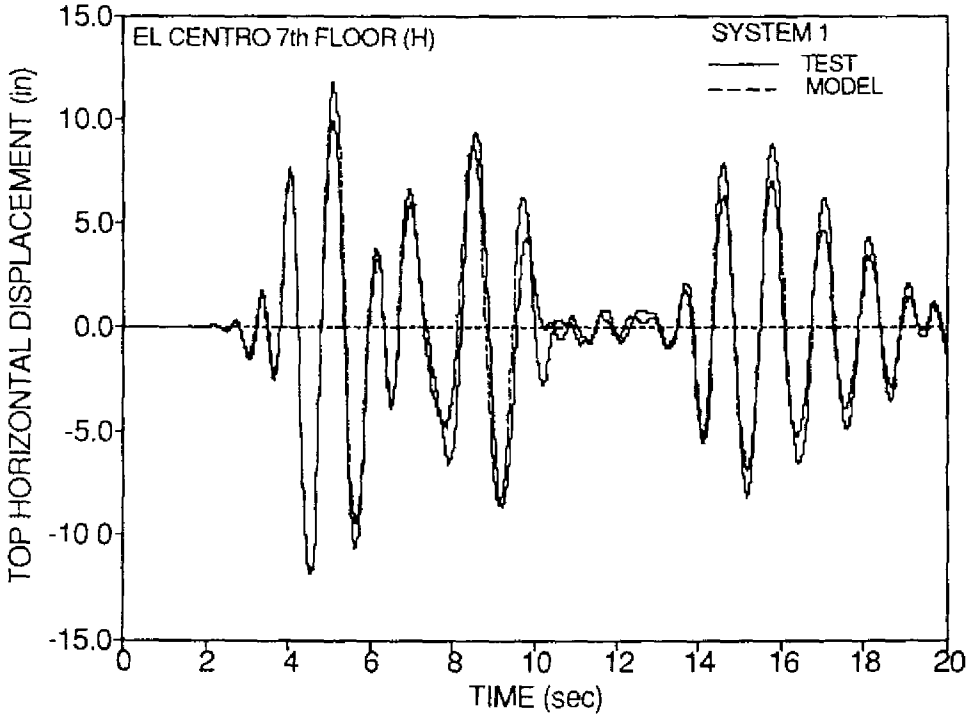

Figure 4-12 Comparison of Experimental and Analytical Time Histories of Horizontal Displacement of Top for El Centro 7th Floor Motion (1 in.= 25.4 mm).

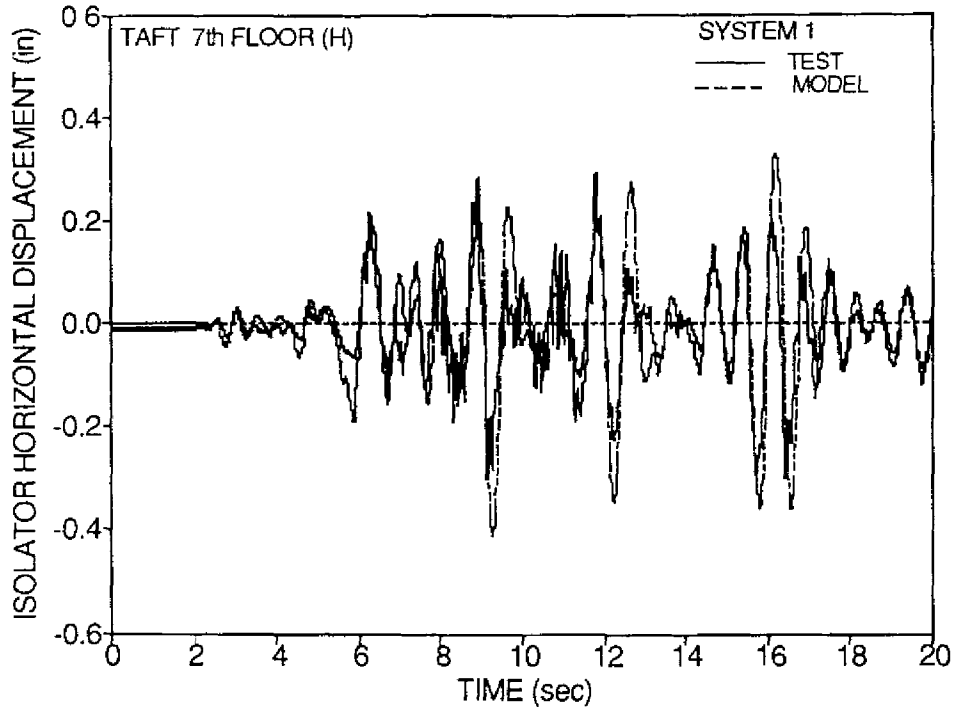

Figure 4-13 Comparison of Experimental and Analytical Time Histories of Horizontal Isolator Displacement for Taft 7th Floor Motion (1 in.= 25.4 mm).

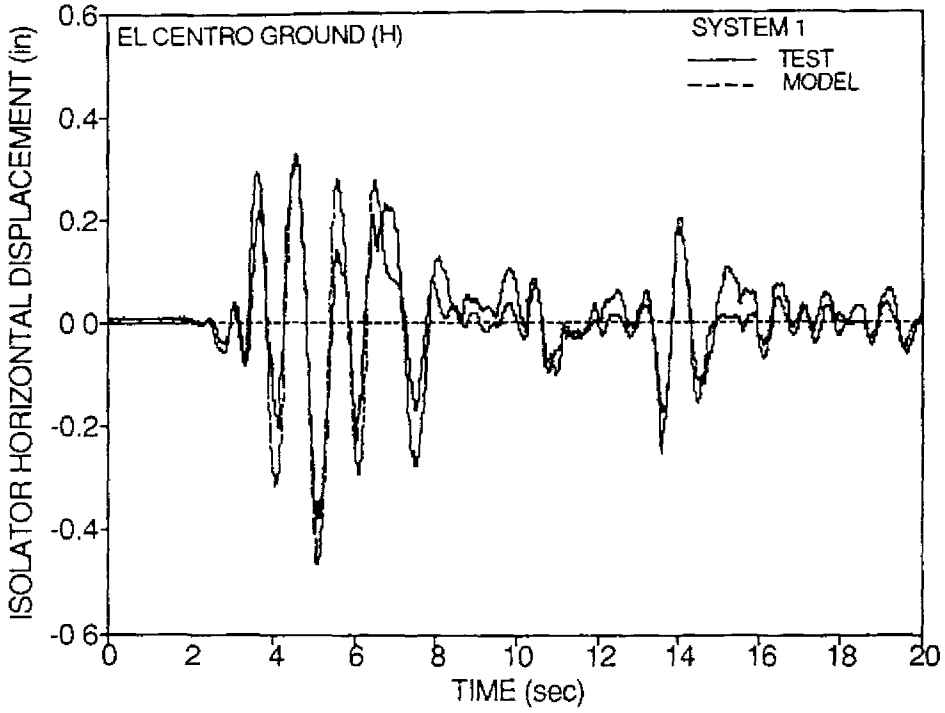

Figure 4-14 Comparison of Experimental and Analytical Time Histories of Horizontal Isolator Displacement for El Centro Ground Motion (1 in.= 25.4 mm).

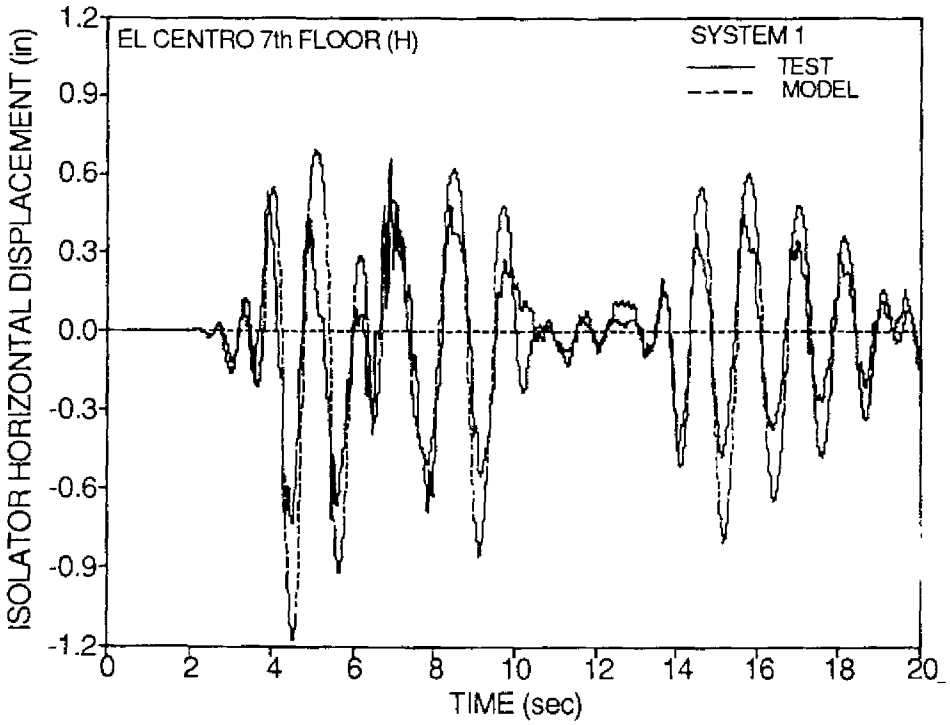

Figure 4-15 Comparison of Experimental and Analytical Time Histories of Horizontal Isolator Displacement for El Centro 7th Floor Motion (1 in.= 25.4 mm).

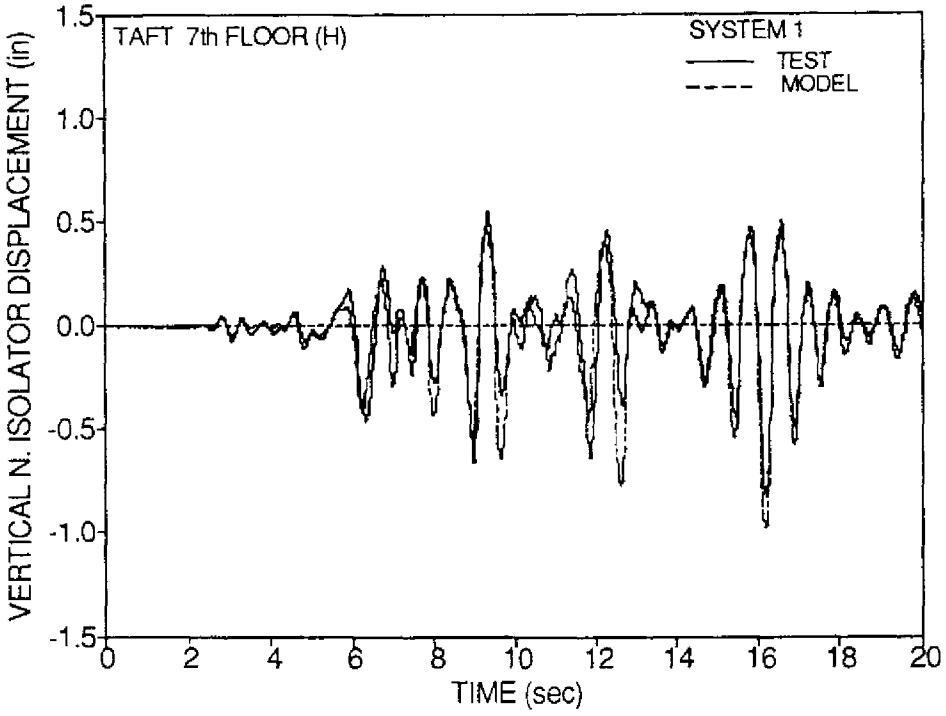

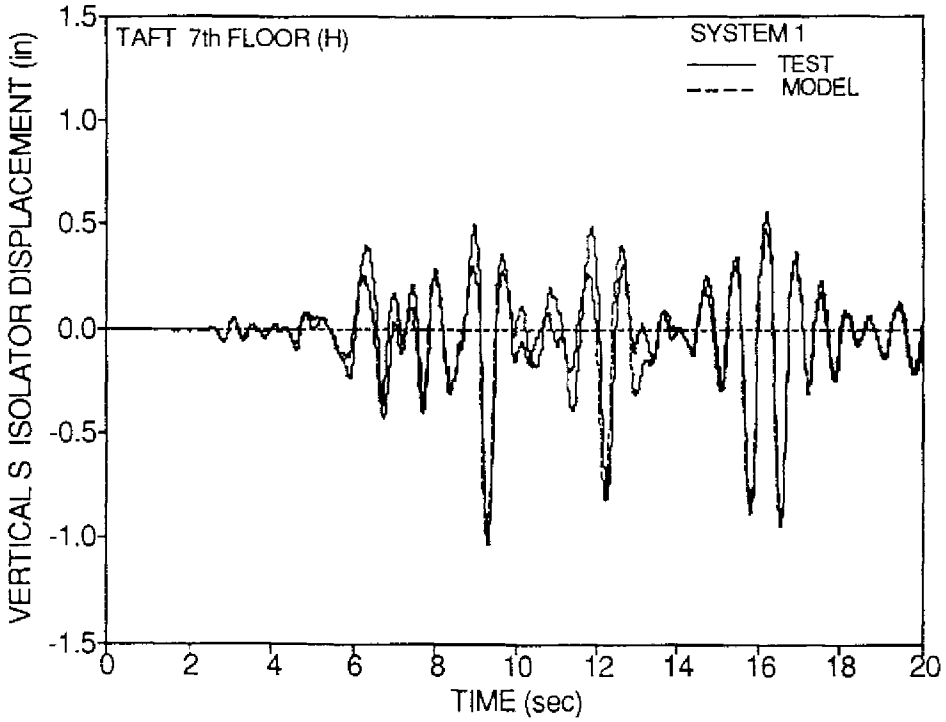

Figure 4-16 Comparison of Experimental and Analytical Time Histories of Vertical Isolator Displacement for Taft 7th Floor Motion (1 in.= 25.4 mm).

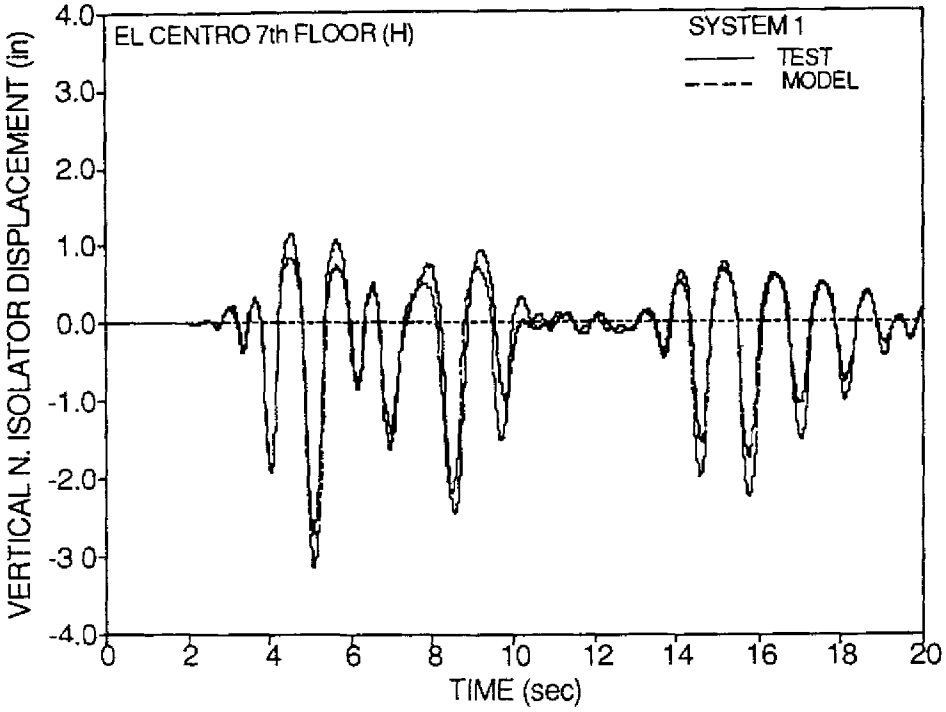

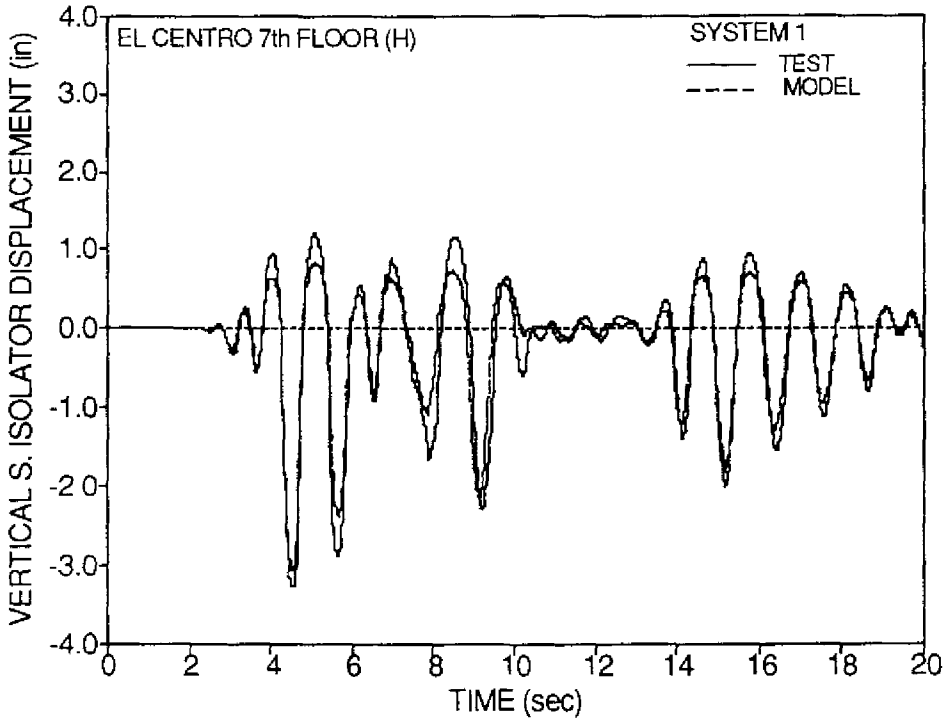

Figure 4-17 Comparison of Experimental and Analytical Time Histories of Vertical Isolator Displacement for El Centro 7th Floor Motion (1 in.= 25.4 mm).

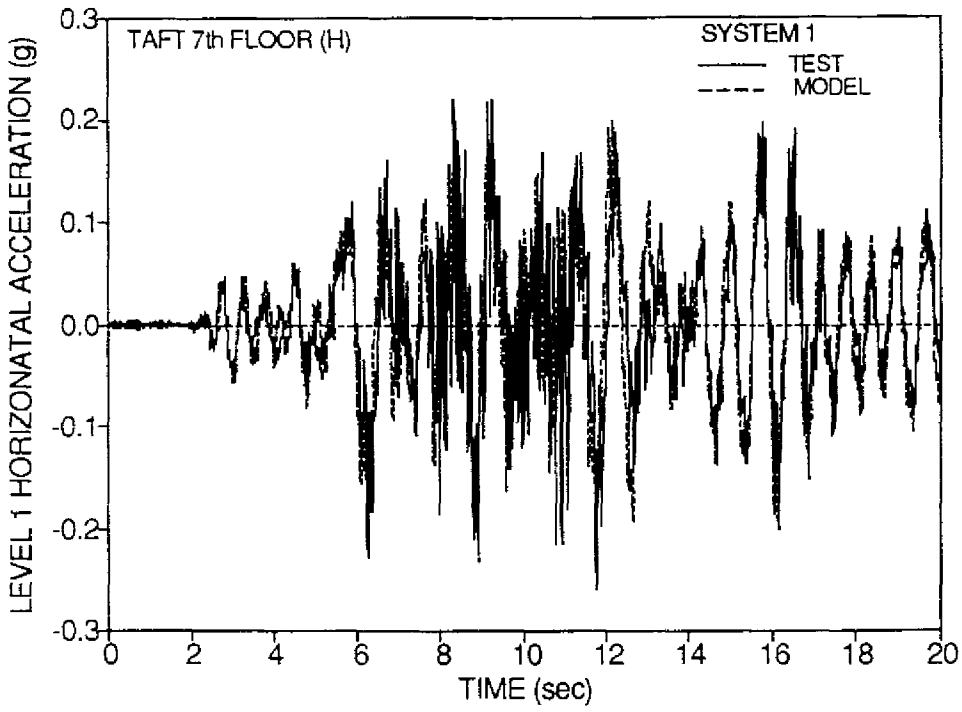

Figure 4-18 Comparison of Experimental and Analytical Time Histories of Horizontal Acceleration of Level 1 for Taft 7th Floor Motion (1 in.= 25.4 mm).

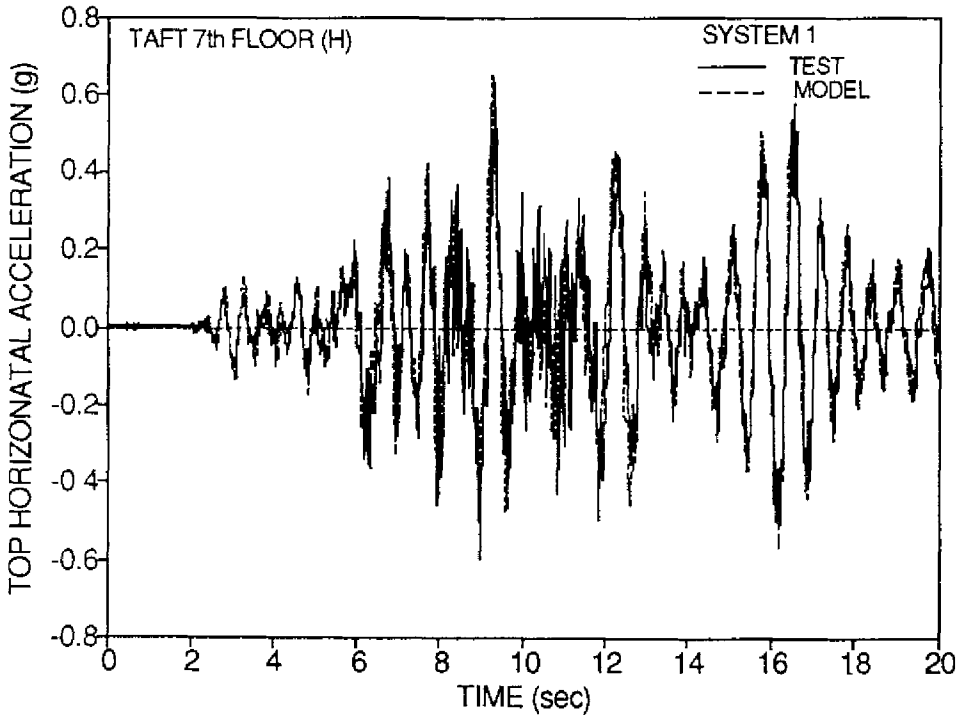

Figure 4-19 Comparison of Experimental and Analytical Time Histories of Top Horizontal Acceleration for Taft 7th Floor Motion (1 in.= 25.4 mm).

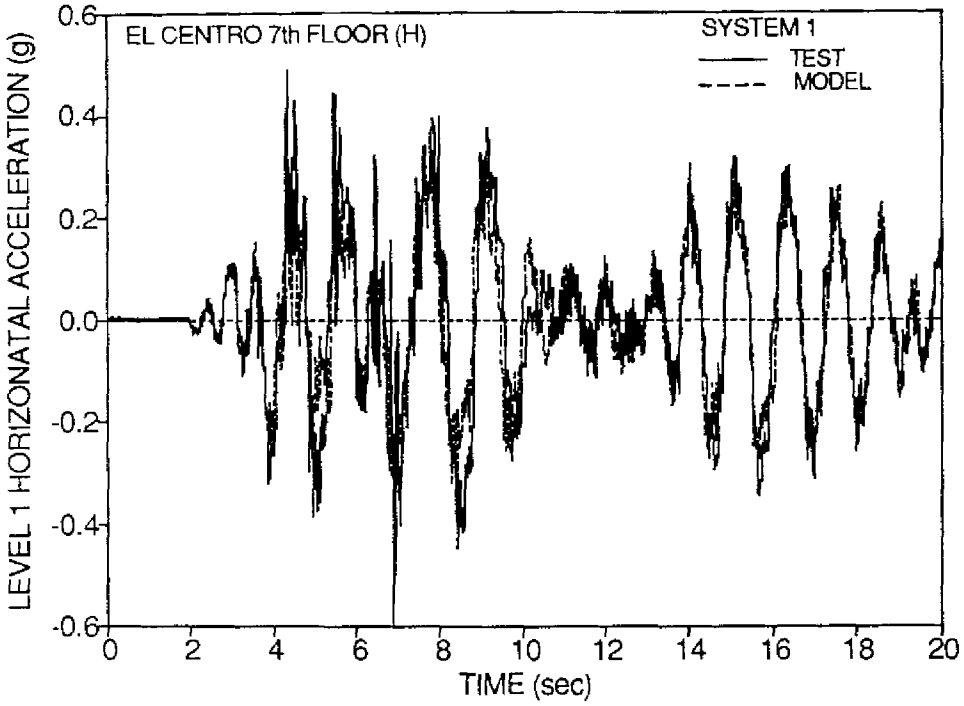

Figure 4-20 Comparison of Experimental and Analytical Time Histories of Horizontal Acceleration of Level 1 for El Centro 7th Floor Motion (1 in.= 25.4 mm).

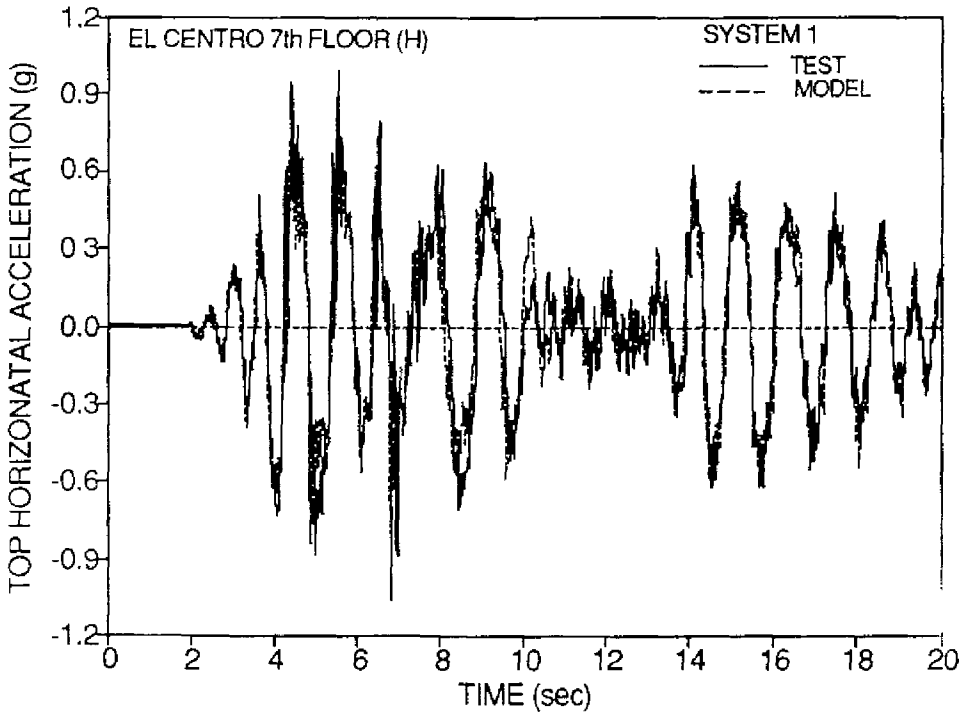

Figure 4-21 Comparison of Experimental and Analytical Time Histories of Top Horizontal Acceleration for El Centro 7th Floor Motion (1 in.= 25.4 mm).

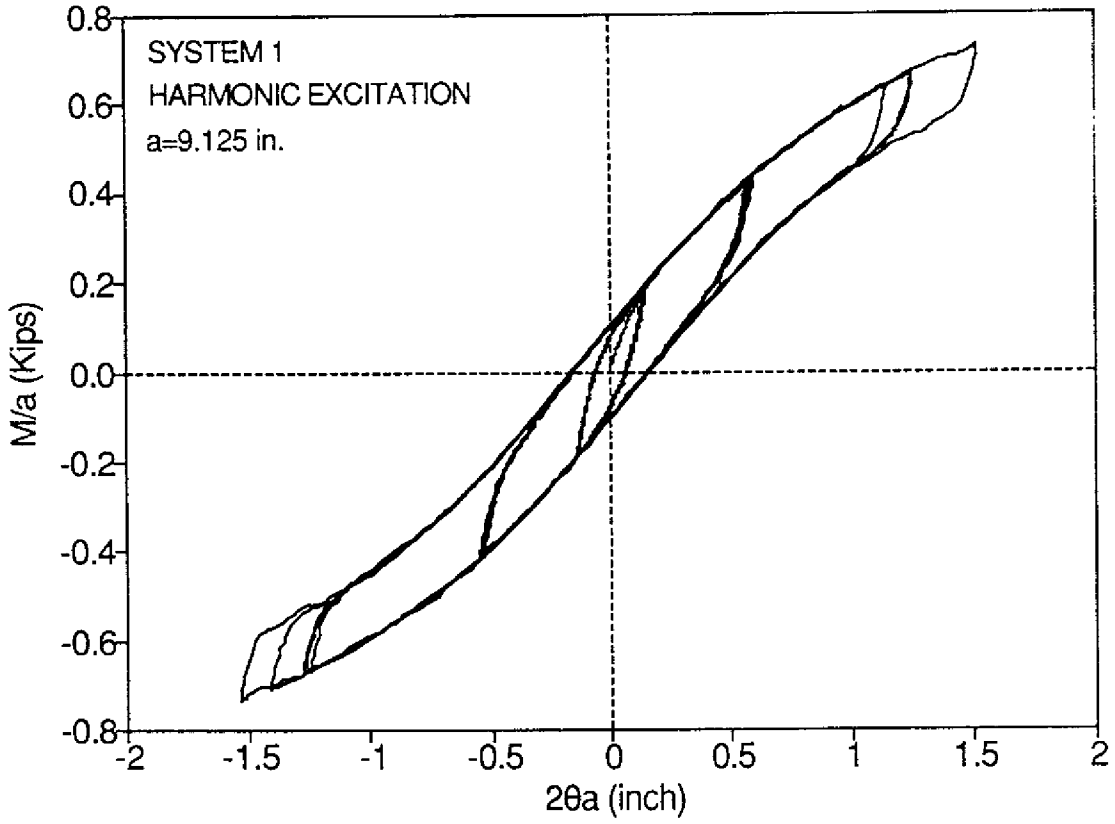

Figure 4-22 Analytical Moment - Rotation Loops of Syste for Harmonic Excitation (1 in.= 25.4 mm, 1 Kip= 4. kN).